ACS APPLIED MATERIALS & INTERFACES

www.acsami.org Research Article

Gas-Cluster Ion-Beam-Assisted Deposition for Fabricating Dry Multilayers Containing Enzyme and Substrate with On-Demand Release

Benjamin Tomasetti, Mehdi Lakhdar, Vincent Delmez, Christine Dupont-Gillain, Clément Lauzin, and Arnaud Delcorte*

Cite This: https://doi.org/10.1021/acsami.4c06432 Read Online

ACCESS | Metrics & More | Article Recommendations | Supporting Information

ABSTRACT: Gas-cluster -beam-assisted deposition is used to build multilayered protein-based structures. In this process, $Ar_{3000-5000}^{+}$ clusters bombard and sputter molecules from a reservoir (target) to a collector, an operation that can be sequentially repeated with multiple targets. The process occurs under a vacuum, making it adequate for further sample conservation in the dry state, since many proteins do not have long-term storage stability in the aqueous state. First of all, the stability in time and versatility in terms of molecule selection are demonstrated with the fabrication of peptide multilayers featuring a clear separation. Then, lysozyme and trypsin are used as protein models to show that the activity remaining on the collector after deposition is linearly proportional to the argon ion dose. The energy per atom (E/n) of the Ar clusters is a parameter that was also changed for lysozyme deposition, and its increase negatively affects activity. The intact detection of larger protein molecules by SDS-PAGE gel electrophoresis and a bioassay (trypsin at ≈25 kDa and glucose oxidase (GOx) at ≈80 kDa) is demonstrated. Finally, GOx and horseradish peroxidase, two proteins involved in the same enzymatic cascade, are successively deposited on β-D-glucose to build an on-demand release material in which the enzymes and the substrate (β-D-glucose) are combined in a dry trilayer, and the reaction occurs only upon reintroduction in aqueous medium.

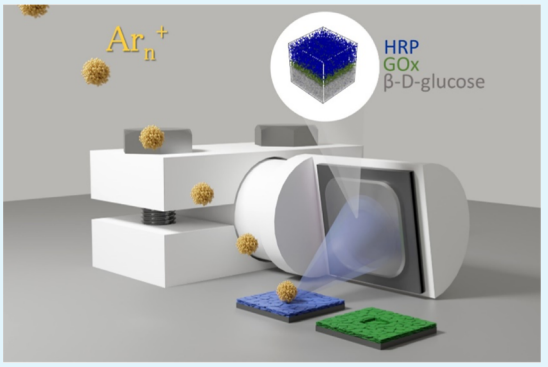

KEYWORDS: *gas cluster ion beam, multilayer, enzymatic cascade, glucose oxidase, lysozyme, trypsin*

INTRODUCTION

New routes for the creation of bioactive organic films hold promise in the development of cutting-edge biomedical applications.[1,2] Proteins serve as crucial building components for such films due to their unique ability to perform enzymatic reactions that are essential for various functions. However, immobilizing proteins onto surfaces poses challenges due to inherent issues of spontaneous adsorption. This process often leads to concerns such as denaturation (altering the protein's 3D structure), which can potentially compromise their bioactivity. Furthermore, the construction of complex multilayer structures comprising diverse biomolecules remains difficult. To overcome these challenges, numerous advanced methodologies have been devised. For example, the layer-by-layer (LbL) techniques involving polyelectrolytes offer a strategy, although it may require nonphysiological pH conditions, leading to multilayer systems.[3,4] However, there are issues such as potential agglomeration and limited applicability across multiple proteins. Indeed, the main driving force for LbL assembly is electrostatic interactions, a parameter hard to control and exhibiting significant variability across different proteins. Within these innovative alternatives, preparative mass spectrometry techniques have emerged as a promising avenue,[5] broadening the scope of possibilities. Methods such as electrospray ionization,[6,7] matrix-assisted laser desorption/ionization (MALDI),[8] and gas cluster ion beam (GCIB)-assisted deposition (iBeam method)[9−11] involve transferring proteins in the ultrahigh vacuum and possibly redepositing them onto a surface. The gentle landing of molecules in a vacuum environment results in the creation of bioactive materials with controlled deposition.

Using GCIB, it is possible to transfer intact molecules from a target to a collector. When the cluster projectiles impact the surface, if the energy per atom (E/n) of the cluster is low enough, the collision induces soft emission, with molecular internal energies precluding fragmentation.[12] If E/n increases, the internal energy and the fragmentation of the sputtered

Received: April 19, 2024
Revised: June 19, 2024
Accepted: June 24, 2024

molecules increase until it reaches a constant level for E/n around 10 eV/atom. Moreover, other cluster parameters influence the desorption efficiency of the GCIB such as the impact angle[11,13] or the cluster size (n), which determine the momentum transmitted to the desorbing molecule.[14,15] These properties make the GCIB a valuable ion source for secondary ion mass spectrometry (SIMS). In addition, a considerable level of sputtered neutral species is increasingly used. The first application of this soft desorption using large argon clusters was to transfer small acidic molecules (MALDI matrices) on samples for in situ matrix-enhanced SIMS (in situ ME−SIMS).[16−18] In parallel, Delmez et al.[10] have shown that biomolecules as large as 14 kDa (lysozyme) could be transferred intact and with retention of their bioactivity, upon reintroduction into solution. Then, the transfer of lipids from a mouse brain tissue to a collector not only allowed to demonstrate that the overall mass spectral signature was preserved upon transfer but also showed that it is possible to increase the ion signal of some lipids after transfer.[19] Therefore, the GCIB-assisted deposition method, coined iBeam, has already demonstrated numerous benefits that can be summarized as follows:[11] (i) the versatility of the chosen deposition surface (collector), (ii) the precise control of the thickness which is proportional to the Ar cluster ion dose used, (iii) the potential to create alternate multilayers using any type of biomolecule, even heavier than 10 kDa, (iv) and the absence of solvent or matrix intermediate that increase the degradation rates by surrounding the proteins molecules.[20] These features pave the way toward the creation of complex multilayer systems containing enzymes and their substrates together.

To achieve that outcome and formulate a comprehensive and applicable method, several essential questions still request answers. How far can we push the complexity boundaries with these multilayers? Can a control be exerted over the protein activity remaining on the collector? Ultimately, is it feasible to extend this approach to larger proteins, potentially allowing an enzymatic cascade to be performed? To answer these questions, the first section focuses on constructing multilayers using molecules around 1 kDa. These molecules were selected because their molecular ions can be detected in ToF−SIMS. The objective of this section is to assess the structure and stability of these multilayers after long storage periods by performing ToF−SIMS depth profiles. The following section will be centered on measuring the remaining activity of proteins (lysozyme and trypsin) after their transfer to a collector. For these measurements, two parameters of the GCIB beam will be manipulated: the total cluster ion dose impacting the target and the energy per atom of the clusters (E/n). Finally, glucose oxidase (GOx) and horseradish peroxidase (HRP), two proteins involved in the same enzymatic cascade, are successively deposited on β-D-glucose in order to build an on-demand release multilayer. β-D-Glucose is the first substrate of the enzymatic cascade. An absorbance measurement and a ToF−SIMS depth profile will be performed first on a bilayer GOx/β-D-glucose and then on a trilayer HRP/GOx/β-D-glucose. The choice of these proteins was motivated by MD simulations that predicted the intact desorption of GOx from an organic film.[21]

EXPERIMENTAL SECTION

Transfers Using Argon Clusters. The transfer experiments were performed using the GCIB source of a TOF·SIMS 5 (ION−TOF GmbH, Münster, Germany) time-of-flight secondary ion mass spectrometer. The instrument is equipped with a Bi-liquid metal ion gun and Ar-GCIB source primary ion sources providing cluster beams oriented at 45° to the surface normal. For the Ar-GCIB source, the selection of the cluster size is done with a Wien filter and a 90° pulsing system allowing to center the mass distribution of the clusters around a specific value (e.g., Ar_{3000}^+ with a full width at half-maximum around 1300 atoms). The argon cluster ion dose was determined by measuring the current of the beam using a Faraday cup close to the target sample, and it will be specified for each experiment in the Results and Discussion section. The target and the collector were fixed on a 3D printed sample holder described elsewhere.[11] A schematic representation can be found in the Figure S1B. Targets can either be powder-deposited onto a tape or as a solution left to dry on a silicon wafer. In both scenarios, they are constructed to be sufficiently thick to not reach the support during the transfer. In the experimental results presented here, a solution was dried on silicon surfaces, with five consecutive depositions of 20 μL from a 20 g/L concentration. The targets were thick (0.73 mm) 4 × 4 mm^2 square silicon wafers. Collectors were silicon wafers cleaned for 15 min in a piranha mixture (sulfuric acid/hydrogen peroxide, 4:1) or PE sheets cleaned for 15 min in an ethanol ultrasonic bath. For GOx transfers on β-D-glucose, 50 μL of a 90 g/L β-D-glucose solution was drop-casted on a cleaned Si wafer.

ToF−SIMS Measurements. The depth profiles were performed on the same instrument as for the deposition via a dual beam method. A 10 keV Ar_{3000}^+ beam was employed to sputter the material with a raster fixed at 600 × 600 μm^2, whereas 30 keV Bi_5^+ ions were used as the analysis beam to record the profiles (current of 0.05 pA for a cycle time of 150 μs). The sputter current was adjusted between 0.07 and 0.22 nA depending on the sample thickness. Charge compensation was conducted using 5 eV electrons. Noninterlaced dual ion beam mode was used. A sputtering time of 1.5 s was applied between each analysis frame, along with a variable pause time based on the sample thickness. Calibration of the mass spectra was performed by using the SurfaceLab software. CH^-, C_3H^-, C_4H^-, and C_6H^- were used in negative mode and CH_3^+, $C_2H_5^+$, $C_3H_5^+$, and $C_4H_7^+$ in positive mode.

Activity Bioassays. The lysozyme activity was tested using the 4-methyllumbelliferyl β-D-N,N′,N″-triacetylchitotrioside compound as substrate. Active lysozyme hydrolyzes one or more glycosidic bonds releasing the fluorescent 4-methylumbelliferyl moiety. 200 μL of distilled water were used to put the lysozyme drop-casted or transferred on the Si collectors back into solution (four successive washing with a drop of 50 μL). A pipet tip was used to scratch the surface to solubilize the maximum amount of protein. These 200 μL were directly put in a 96-well opaque microplate. Then, 20 μL of 4-methylumbelliferyl β-D-N,N′,N″-triacetylchitotrioside (0.1 g/L, Steinheim, Germany) in dimethyl sulfoxide/water 2:1 (v/v) solution were added as lysozyme substrate in each well. The fluorescence was measured after 24 h of incubation at 40 °C using a SPECTROMAX id3 microplate reader (excitation/emission = 360/450). Lysozyme was purchased from ThermoFischer (89,833, ±20,000 units/mg) and from Sigma-Aldrich (L6876, ±40,000 units/mg) and used without further purification.

The enzymatic activity of trypsin was measured using the Thermo Scientific Pierce Fluorescent Protease assay kit (ref 23,266) including a fluorescein-labeled casein. Fluorescence was measured after 50 min of incubation at room temperature using a SPECTROMAX id3 microplate reader (excitation/emission wavelengths = 485 nm/538 nm). The calibration curve was performed by letting dry increasing known amounts of trypsin on silicon wafers. Then 100 μL of buffer were used to put back the protein in solution within each well of a microplate. The same volume was used to recover the proteins from the transferred samples. The stock of used trypsin was a lyophilized powder (97%) having an activity of 309 TAME units/mg of protein.

The enzymatic activity of GOx was measured by using the Megazyme assay kit. This protein is involved with HRP in the following enzymatic cascade

https://doi.org/10.1021/acsami.4c06432
ACS Appl. Mater. Interfaces XXXX, XXX, XXX−XXX

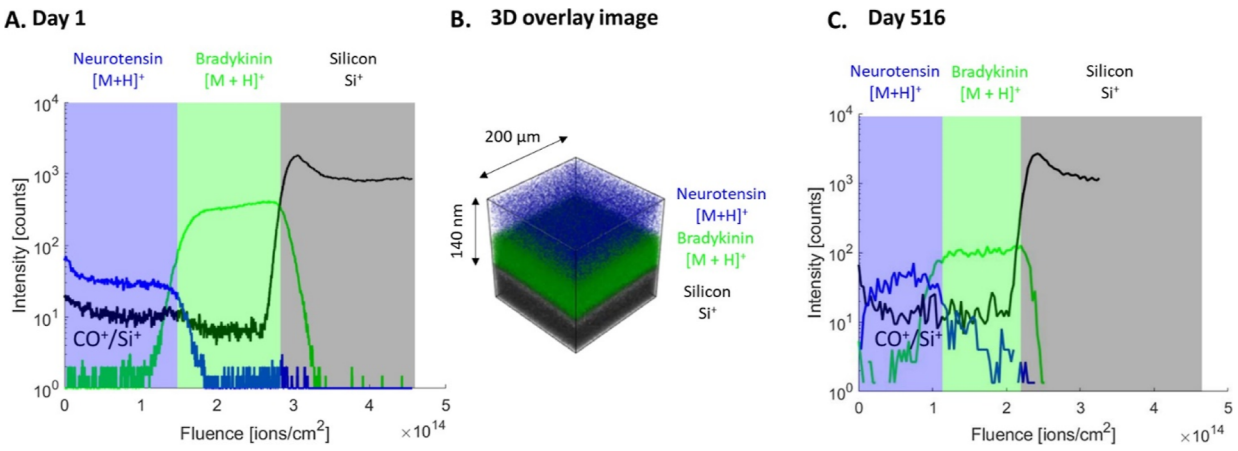

Figure 1. Positive depth profile (A) and reconstructed 3D SIMS image (B) of a bilayer constructed by successive transfers of bradykinin and neurotensin (5×10^{14} ions of 10 keV Ar_{3000}^+ beam). The thickness of the bilayer (140 nm) was measured by profilometry using the crater induced by the depth profile. (C) Positive depth profile conducted 516 days after the bilayer fabrication, during which the sample was stored in a drawer without any additional specific care.

$$\beta - \text{D} - \text{glucose} + \text{O}_2 + \text{H}_2\text{O} \xrightarrow{(\text{GOx})} \text{D} - \text{glucono} - \delta - \text{lactone} + \text{H}_2\text{O}_2 \quad (1)$$

$$2\text{H}_2\text{O}_2 + p - \text{hydroxybenzoic acid} + 4 - \text{aminoantipyrine} \xrightarrow{(\text{HRP})} \text{quinoneimine dye} + 4\text{H}_2\text{O} \quad (2)$$

The quantitative formation of the quinoneimine dye complex was measured by absorbance. The difference between the absorbance after 20 min of reaction and at the beginning ($\Delta A_{510\text{nm}}$/20 min) was measured at 510 nm using a SPECTROMAX id3 microplate reader. GOx used for the target and the transfers is from Sigma-Aldrich (49,180, ±200 units/mg) and was used without further purification. If GOx was directly transferred on the support, collectors in PE could be used and were directly wrapped in the microplate wells. The presence of the PE sample does not affect the linearity of the absorbance measurements (see Figure S5). For GOx transferred on a layer of β-D-glucose, silicon collectors were used and 100 μL of distilled water was used to solubilize GOx and glucose (two successive washings with a drop of 50 μL each). The other molecules needed for the enzymatic cascade came from the addition of 200 μL of the kit mixture (containing the HRP + *p*-hydroxybenzoic acid +4-aminoantipyrine + preservatives). For the HRP/GOx/β-D-glucose trilayer, GOx and HRP were both transferred using argon clusters on a layer of β-D-glucose. HRP (P8125, ≥50 units/mg) and 4-aminoantipyrine (A4382) were bought from Sigma-Aldrich. 100 microliters of distilled water were used to solubilize the trilayer. 200 microliters of a buffer containing *p*-hydroxybenzoic acid and 0.625 g/L of 4-aminoantipyrine were added.

SDS-PAGE Gel Electrophoresis. SDS-PAGE was performed in 4−20% iD polyacrylamide gel. 50 microliters of water were used to solubilize the proteins from the collector and 10 μL of Laemmli buffer (without DithioThreitol) were added. The solution was then heated for 15 min in a warm bath at 56 °C and centrifuged for 1 min. The current of the electrophoresis cell was set at 55 mA, and the cell was filled with a 1× MOPS running buffer. Prestained Protein Ladder (Thermoscientific, USA) was loaded as molecular weight markers. Protein detection was performed using a colloidal Coomassie Blue staining protocol (see in the Supporting Information).

RESULTS AND DISCUSSION

Multilayer Construction and Stability. Multilayer construction using large argon clusters ions has already been achieved.[11] Here the purpose is to explore the limits of these multilayers concerning aging and molecular diversity. First, a bilayer of two peptides, both soluble in water, was built. Targets of bradykinin and neurotensin were successively bombarded with a 10 keV Ar_{3000}^+ beam with a dose of 5×10^{14} ions each. Figure 1A,B show the positive depth profile and its 3D reconstruction performed on the bilayer after the transfers. The profile shows that the peptide layers feature a clear separation. Indeed, the molecular signal $[M + H]^+$ of neurotensin significantly decreases within the bradykinin layer, and vice versa. The sputtering rate of these two peptides should be close since they have comparable masses (1673 Da for neurotensin and 1060 Da for bradykinin); thus, the thickness of both layers should be comparable because the same cluster ion dose was used for the transfers. In positive mode, the mass resolving power at m/z 28 (Si^+) is around 5000, which is not sufficient to totally resolve the CO^+ ions coming from the organic layer from the Si^+ ions. This is why there is a plateau of Si^+ in the peptide layers in the positive mode. The negative depth profile is available in Figure S2. Figure 1C shows the same depth profiling conducted 516 days after the bilayer construction, during which the sample was preserved without any specific conditions (ambient atmosphere). The fluence required to reach the silicon layer in the profile varies a little because the local thickness of the deposit is influenced by the angular distribution of the molecules, making it slightly thicker at the center and thinner at the edges.[11] The profile on day 1 was performed at the center of the collector, whereas the profile on day 516 was performed at some distance. After that storage period, the bilayer retained its integrity with three distinct zones. However, there is a decrease of the neurotensin molecular signal at the surface and an increase of the CO^+/Si^+ signal. This indicates a change of composition at the surface that might result from deposition of other organic molecules (contamination) or from the peptides' degradation. A common contaminant observed in ToF−SIMS spectra is poly dimethylsiloxane (PDMS) that contaminates sample surfaces by simple exposure to laboratory air.[22] After 516 days, the intensities of two prominent peaks of PDMS, Si^+ and $Si_2O_2C_5H_{15}^+$ (m/z 147), increased at the sample surface. Moreover, there is also a decrease in the bradykinin signal $[M + H]^+$ in the bulk. Despite the signs of peptide degradation, it is worth noting that most decomposition reactions should be slowed in the dry state. Indeed, these reactions are minimal at or below the monolayer level of hydration because the lower

https://doi.org/10.1021/acsami.4c06432
ACS Appl. Mater. Interfaces XXXX, XXX, XXX−XXX

amount of adsorbed water reduces the conformational flexibility of the peptide/protein and limits the mobility of reactants.[20,23] This experiment shows that the GCIB-assisted layer deposition method provides two advantages compared to other building methods. First, the process operates under vacuum conditions, potentially enhancing the pharmaceutical stability of the final product due to reduced water content. Second, reactive compounds can be brought into close contact and deactivated until a substantial amount of solvent is introduced into the system.

To validate the versatility of the method regarding molecule selection and transfer, depth profiles were performed on a trilayer composed of neurotensin, IRGANOX 1010 and bradykinin (Figures S3 and S4). IRGANOX 1010 is an antioxidant and polymer additive with a low solubility in water compared to those of the other two peptides. Each layer was deposited using the same dose of 3×10^{14} ions of a 10 keV Ar_{3000}^{+} beam. Depth profiles conducted on day 1 and after a storage period of 611 days reveal a clear demarcation between each layer, indicating that time has not impacted their delineation. The molecular ion signal intensity of each molecule decreases over time due to inevitable degradation reactions, even in the dry state. However, separated unfragmented molecules are still detected. This outcome indicates that numerous multilayer arrangements are feasible. Moreover, since the quantity of molecules within each layer is proportional to the Ar ion dose used for the transfer,[11] it enhances the potential utility of this approach. Subsequently, the upcoming sections aim to study the transfer of proteins and investigate the feasibility of establishing bioactive multilayer systems.

Control of the Enzymatic Activity. It was shown that lysozyme can be transferred intact on a collector and that the protein is active when it goes back into solution.[10] However, this result was obtained with a transfer geometry that was not optimal (Figure S1A), corresponding to an exceedingly long transfer duration to obtain only an activity level roughly equivalent to that of 0.9 μg of fresh lysozyme. Following this result, three objectives were targeted in this section: (i) Demonstrate that utilizing the new sample holder with an impinging angle of 45° (Figure S1B) allows one to achieve higher activity levels more effectively. (ii) Show that the activity of the collector could be finely controlled with the Ar cluster ion dose. (iii) Explore the feasibility of transferring proteins of higher masses by reducing the energy per atom of the cluster or increasing the transfer time.

For this purpose, fluorescence-based enzymatic activity assays were performed on the collector after several transfers of increasing dose. This experiment was performed for two proteins, lysozyme (≈14 kDa) and trypsin (≈25 kDa). Figure 2 shows that the measured fluorescence increases linearly with the Ar cluster ion dose for both proteins. For these bioassays, a calibration was performed using drop-cast proteins on Si wafers (Figure S5). The drop-casting of fresh lysozymes and trypsin was used to mimic the collectors that are obtained after the transfers. Indeed, as described in the Experimental Section, a small volume of buffer was used to solubilize the collected proteins. During this step, it is expected that at least a monolayer of protein material will remain attached to the collector and will no longer participate in the enzymatic reaction. This hypothesis is confirmed by comparing the calibration of the drop-casted layer (Figure S5) with a direct calibration, for which all of the proteins participate in the enzymatic reaction. Moreover, a 3D mapping of the thickness of the protein layer remaining on the Si collector shows that a monolayer, approximately 2−3 nm in thickness, is adsorbed at the surface of the collector after solubilization (Figure S6).

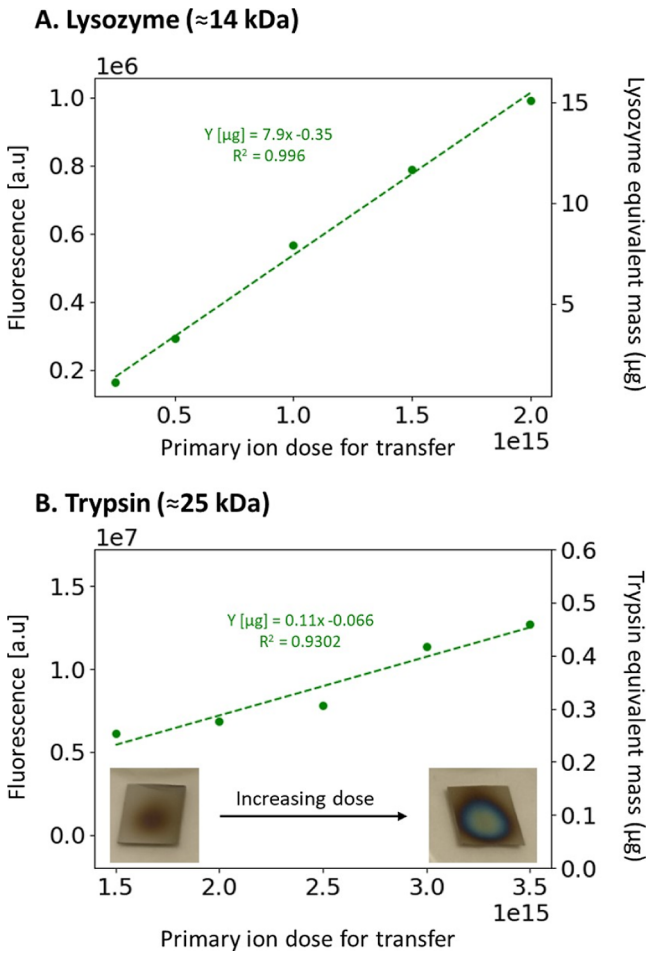

Figure 2. (A) Lysozyme and (B) trypsin fluorescence measurements for several transfers at different doses. Every dot represents a distinct collector for which the material was redissolved to conduct the bioassay. The pictures show the collectors after the transfer of trypsin with a dose of 1.5×10^{15} ions and 3.5×10^{15} ions.

The term "equivalent mass" is employed on the right axis of the plots in Figure 2. This term "equivalent" is utilized because it is likely that the specific activity could differ between the reference proteins used for the calibration and the transferred proteins. Indeed, slight composition changes are induced by the transfer due to fragmentation but also differential sputtering that may occur between the protein and the impurities. Moreover, it is highly possible that the proteins unfold upon the impact with the Ar cluster (hypothesis supported by MD simulations for lysozyme).[24] The protein unfolding may expose amino acid residues, which could facilitate further inactivation such as aggregation and chemical modification. However, protein unfolding is a reversible process.[25,26] Even if the reduced amount of water and the collision tend to shift the equilibrium between native and unfolded toward unfolded, some of the transferred proteins may fold back once in solution. Considering these comments are considered, the trypsin and lysozyme equivalent masses that were deposited cannot be quantitatively compared. Moreover, the activity of the protein-covered collector will

https://doi.org/10.1021/acsami.4c06432
ACS Appl. Mater. Interfaces XXXX, XXX, XXX−XXX

depend on the purity and initial activity of the reference protein used for the target.

SDS-PAGE gel electrophoresis was previously used to confirm the presence of unfragmented lysozymes on the collector.[10] To be sure that the trypsin is also transferred intact (in native and/or unfolded conformation), a SDS-PAGE was also performed and can be found in Figure S7. Using a 10 keV Ar_{5000}^+ beam with a dose of 2.1×10^{15} ions, a thin band was visible at the same position as the reference (≈25 kDa), indicating the presence of unfragmented trypsin on the collector.

The correlation between fragmentation and energy per atom (E/n) of the Ar clusters is well-established. It was previously demonstrated for peptides that an increase in E/n induces more fragmentation, resulting in decreased detection of intact peptides after transfer.[11] To investigate the hypothesis that a more fragmented transferred protein may experience a decline in activity, lysozyme (±40,000 units/mg) was transferred with different beam conditions. The findings, presented in Table 1,

Table 1. Fluorescence Measured from Lysozyme Transferred upon Beam of Decreasing Energy per Atom

Cluster Beam	Current (nA)	Ion dose (ions)	Energy per Atom (eV/atom)	Fluorescence (R.F.U)
10 keV Ar_{1500}^+	14.2	2x10^{15}	6.67	2.86x10^5
10 keV Ar_{3000}^+	9.4	2x10^{15}	3.33	3.78x10^5
10 keV Ar_{5000}^+	2.1	2x10^{15}	2	5.03x10^5

confirm that a higher E/n, under the same ion dose, correlates with a reduction in activity, as measured by fluorescence. This reduction of activity is observed even if clusters featuring a higher E/n value favor desorption and display higher deposition rate.[11]

It is important to highlight that while beams with higher E/n induce greater fragmentation, the significantly reduced transfer time, due to a higher beam current, enables the rapid attainment of higher activity levels in the samples. To reach a cluster ion dose of 2×10^{15} ions with a 10 keV Ar_{3000}^+ beam (9.4 nA), the sputtering lasts 9.5 h. At this point, enzyme-based structures have been created, with their activity precontrolled by the transfer dose.

Toward Larger Protein Transfer and On-Demand Release Multilayers. In this section, the objective is to investigate the real potential benefits of GCIB assisted deposition as a solvent-free method, enabling the integration of enzymes and their substrates into a dry multilayer.

The first step was to confirm the presence of intact GOx molecules (≈80 kDa) on the collector. SDS-PAGE electrophoresis was conducted on the transferred material (Figure S7). After several failures to detect a band at the same mass as the reference, a high dose of 10 keV Ar_{3000}^+ beam (4.03×10^{16} ions) was used for the transfer. With the current performance of the GCIB source, it represents a transfer time of about 185 h. It demonstrates a low transfer efficiency for such a large protein, potentially due to high levels of fragmentation. However, the limit of detection of the Megazyme assay kit is low (linear range between 0.01 and 0.08 U/mL) allowing us to work with this enzyme within a feasible time frame.

Therefore, GOx was deposited on a layer of β-D-glucose to build an enzyme/substrate bilayer in a vacuum. First, the β-D-glucose was drop-cast on silicon (50 μL at 90 g/L). β-D-glucose could also be transferred, but due to the large amount needed (4.5 mg per microplate well) and to ensure that only the enzymes are dependent on the argon dose, the first layer was drop-casted. Then, GOx was deposited on top of this layer using 3×10^{15} ions of a 10 keV Ar_{5000}^+ beam. Figure 3A shows

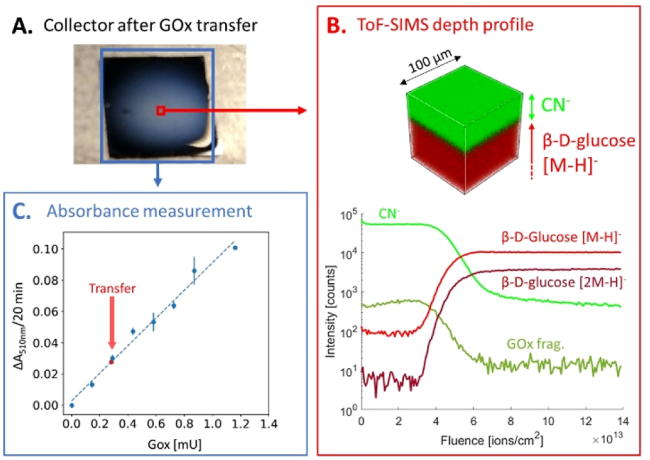

Figure 3. (A) Picture of the collector coated with a bilayer consisting of a layer of drop-casted β-D-glucose and a layer of transferred GOx (3×10^{15} ions of 10 keV Ar_{5000}^+ beam). (B) ToF–SIMS depth profile performed in the center of the sample. (C) Absorbance measurement after solubilization of the collector (red) and the corresponding calibration (blue).

a picture of the bilayer after deposition of GOx. The white smear visible on the top corresponds to the deposited GOx. The glucose is the underneath translucid layer. Figure 3B shows a depth profile performed in the center of the sample. The GOx layer (as revealed by the signal of the CN^- fragment) is well separated from the β-D-glucose layer. Another ion originating from the GOx sample is plotted (called the GOx frag.) This fragment, with a m/z value of 127.96, could correspond to either $C_4H_2S_2N^-$ or $C_5H_4S_2^-$ with deviations of 8 and 90 ppm, respectively. This ion remains unassigned due to the uncertainty on its mass assignment. Nevertheless, it later served as a marker for the GOx layer. Both layers are clearly distinguishable, with no indication of reaction occurring at their interface. The observed plateau of β-D-glucose $[M - H]^-$ within the protein layer arises from interferences of ions with closely matching masses. However, the mass resolution of the instrument prevents differentiation of these contributions. After acquisition of the profile, the collector content was solubilized with 100 μL of distilled water and the absorbance was measured using the Megazyme protocol (see the Experimental Section). Figure 3C shows the $\Delta A_{510\ nm}/20$ min measurement of the transferred layer and compares it with a calibration obtained with free GOx in solution. This absorbance is equivalent to 0.28 mU of GOx used for the calibration. The experiment was reproduced twice, resulting in 0.10 ± 0.01 mU for every 10^{15} bombarded cluster ions. Then, the same bilayer GOx/β-D-glucose was fabricated twice but using a 10 keV Ar_{3000}^+ beam to deposit the GOx. The result is found in the Figure S8. A higher dose of 4.39×10^{15} ions was used, resulting in a thicker deposition. However, even if the dose was higher than in the result of Figure 3, the measured absorbance is equivalent to 0.021 ± 0.011 mU for every 10^{15} bombarded cluster ions. It shows once again that E/n is an important parameter.

https://doi.org/10.1021/acsami.4c06432
ACS Appl. Mater. Interfaces XXXX, XXX, XXX−XXX

To progress further and particularly to move closer to a multilayer with on-demand release capabilities, both enzymes were transferred successively on the first substrate (β-D-glucose). Figure 4B,C shows the depth profile and the absorbance measurement. The depth profile was normalized by the total ion count due to small fluctuations of the bismuth analysis beam current at the beginning of the profile. Two arbitrary ions (HRP frag. at m/z 368.86 and GOx frag. at m/z 127.96) were chosen to distinguish both layers. A small variation in the CN^- ion intensity can be detected between both layers. After acquisition of the profile, the layer on the collector was solubilized using 200 μL of a buffer containing *p*-hydroxybenzoic acid and 4-aminoantipyrine (0.625 g/L). The reaction began directly as all the components needed for the enzymatic cascade were present. The $\Delta A_{510\ nm}$/20 min is equivalent to 0.22 mU of the GOx used for calibration. This amount is close to that measured with the bilayer. This was expected, as the doses used for the transfer of the GOx were close. Moreover, it is assumed that the amount of transferred HRP is sufficiently large and that its final amount in the bilayer is not the limiting factor of the cascade. To support this hypothesis, the $\Delta A_{510\ nm}$/20 min was measured for decreasing amounts of HRP, added from diluted solutions. The absorbance measurement is not affected by the amount of HRP until it decreases to 10 ng by microplate well (Figure S9).

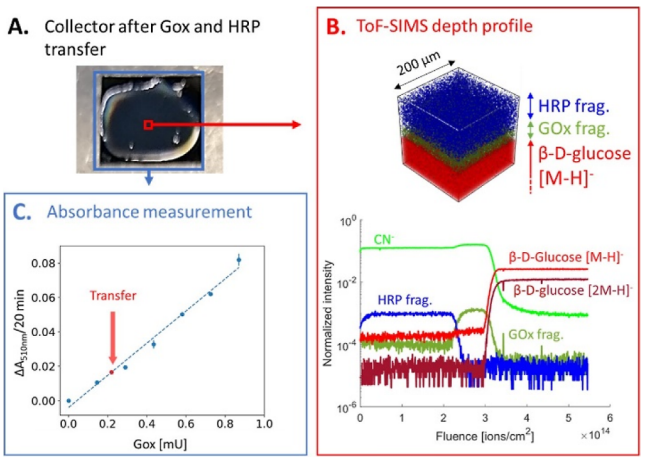

Figure 4. (A) Picture of the collector coated with a trilayer consisting of a layer of drop-casted β-D-glucose, a layer of transferred GOx (3.10×10^{15} ions of 10 keV Ar_{5000}^+ beam) and a layer of transferred HRP (3.39×10^{15} ions of 10 keV Ar_{5000}^+ beam). (B) ToF−SIMS depth profile performed in the center of the sample. (C) Absorbance measurement after solubilization of the collector (red) and the corresponding calibration (blue).

CONCLUSIONS AND FUTURE PROSPECTS

This study presents the fabrication of on-demand release multilayers composed of proteins using GCIB-assisted deposition. The method has demonstrated the ability to construct multilayers of distinct molecules without mixing and without the use of solvents. The equivalent activity of the collector, the newly constructed bioactive material, has been demonstrated to be proportional to the Ar ion dose for two different proteins, lysozyme and trypsin. Moreover, relatively large proteins such as GOx (≈80 kDa) can be deposited unfragmented and show bioactivity when placed in solution. Multilayers composed of two enzymes involved in an enzymatic cascade were deposited on the first layer of substrate. The deposition in a vacuum led to an artificially inactivated stack of molecules. As a result, the reaction was shown to start when the stack was reintroduced in solution.

Future prospects may involve the study of the sticking force or leaching speed of a multilayer, which may differ from other methods, such as LbL or spontaneous adsorption. Finally, the stability of large proteins in the solid state after the transfer should be assessed and compared with other fabrication methods.

ASSOCIATED CONTENT

Supporting Information

The Supporting Information is available free of charge at https://pubs.acs.org/doi/10.1021/acsami.4c06432.

Sample holders schematic representation; positive and negative depth profiles of a bilayer (bradykinin, neurotensin); positive depth profile of a trilayer (bradykinin, IRGANOX, neurotensin) on day 1 and day 611; negative depth profile of a trilayer (bradykinin, IRGANOX, neurotensin) on day 1 and day 611; calibration curves for lysozyme, trypsin and GOx; SDS-PAGE electrophoresis gels for lysozyme, trypsin and GOx; thickness mapping of the collector after solubilization; depth profile and bioassay of a bilayer GOx/β-D-glucose after Ar_{3000}^+ transfers; and absorbance measured for increasing amount of HRP (PDF)

AUTHOR INFORMATION

Corresponding Author

Arnaud Delcorte − *Institute of Condensed Matter and Nanosciences—Université catholique de Louvain, Louvain-la-Neuve 1348, Belgium;* orcid.org/0000-0003-4127-8650; Email: arnaud.delcorte@uclouvain.be

Authors

Benjamin Tomasetti − *Institute of Condensed Matter and Nanosciences—Université catholique de Louvain, Louvain-la-Neuve 1348, Belgium;* orcid.org/0009-0008-7986-6144

Mehdi Lakhdar − *Institute of Condensed Matter and Nanosciences—Université catholique de Louvain, Louvain-la-Neuve 1348, Belgium*

Vincent Delmez − *Institute of Condensed Matter and Nanosciences—Université catholique de Louvain, Louvain-la-Neuve 1348, Belgium;* orcid.org/0000-0002-9203-9919

Christine Dupont-Gillain − *Institute of Condensed Matter and Nanosciences—Université catholique de Louvain, Louvain-la-Neuve 1348, Belgium;* orcid.org/0000-0002-6153-4044

Clément Lauzin − *Institute of Condensed Matter and Nanosciences—Université catholique de Louvain, Louvain-la-Neuve 1348, Belgium;* orcid.org/0000-0001-5044-5137

Complete contact information is available at: https://pubs.acs.org/10.1021/acsami.4c06432

Notes

The authors declare no competing financial interest.

https://doi.org/10.1021/acsami.4c06432
ACS Appl. Mater. Interfaces XXXX, XXX, XXX−XXX

ACKNOWLEDGMENTS

The authors acknowledge the financial support by the Fédération Wallonie Bruxelles, through the project "iBEAM" funded by its research program "Actions de Recherche Concertées" (Convention no. 18/23-090) and by the Belgian National Foundation for Scientific Research (FNRS). B.T. is a research fellow (ASP) of the FNRS. A.D. is a research director of the FNRS. The authors acknowledge Joseph Nader and Louis Gueuning for their help with the SDS-PAGE gel electrophoresis.

REFERENCES

(1) Lu, Y.; Aimetti, A. A.; Langer, R.; Gu, Z. Bioresponsive Materials. *Nat. Rev. Mater.* **2016**, *2* (1), 1−17.
(2) Kitsara, M.; Tassis, G.; Papagiannopoulos, A.; Simon, A.; Agbulut, O.; Pispas, S. Polysaccharide-Protein Multilayers Based on Chitosan-Fibrinogen Assemblies for Cardiac Cell Engineering. *Macromol. Biosci.* **2022**, *22* (1), 2100346.
(3) Vander Straeten, A.; Bratek-Skicki, A.; Jonas, A. M.; Fustin, C. A.; Dupont-Gillain, C. Integrating Proteins in Layer-by-Layer Assemblies Independently of Their Electrical Charge. *ACS Nano* **2018**, *12* (8), 8372−8381.
(4) Vranckx, C.; Lambricht, L.; Préat, V.; Cornu, O.; Dupont-Gillain, C.; Vander Straeten, A. Layer-by-Layer Nanoarchitectonics Using Protein-Polyelectrolyte Complexes toward a Generalizable Tool for Protein Surface Immobilization. *Langmuir* **2022**, *38*, 5579−5589.
(5) Verbeck, G.; Hoffmann, W.; Walton, B. Soft-Landing Preparative Mass Spectrometry. *Analyst* **2012**, *137* (19), 4393−4407.
(6) Ouyang, Z.; Takáts, Z.; Blake, T. A.; Gologan, B.; Guymon, A. J.; Wiseman, J. M.; Oliver, J. C.; Davisson, V. J.; Cooks, R. G. Preparing Protein Microarrays by Soft-Landing of Mass-Selected Ions. *Science* **2003**, *301* (5638), 1351−1354.
(7) Gunaratne, K. D. D.; Prabhakaran, V.; Ibrahim, Y. M.; Norheim, R. V.; Johnson, G. E.; Laskin, J. Design and Performance of a High-Flux Electrospray Ionization Source for Ion Soft Landing. *Analyst* **2015**, *140* (9), 2957−2963.
(8) Räder, H. J.; Rouhanipour, A.; Talarico, A. M.; Palermo, V.; Samorì, P.; Müllen, K. Processing of Giant Graphene Molecules by Soft-Landing Mass Spectrometry. *Nat. Mater.* **2006**, *5* (4), 276−280.
(9) Delcorte, A.; Delmez, V.; Dupont-Gillain, C.; Lauzin, C.; Jefford, H.; Chundak, M.; Poleunis, C.; Moshkunov, K. Large Cluster Ions: Soft Local Probes and Tools for Organic and Bio Surfaces. *Phys. Chem. Chem. Phys.* **2020**, *22* (31), 17427−17447.
(10) Delmez, V.; Degand, H.; Poleunis, C.; Moshkunov, K.; Chundak, M.; Dupont-Gillain, C.; Delcorte, A. Deposition of Intact and Active Proteins in Vacuo Using Large Argon Cluster Ion Beams. *J. Phys. Chem. Lett.* **2021**, *12* (2), 952−957.
(11) Delmez, V.; Tomasetti, B.; Daphnis, T.; Poleunis, C.; Lauzin, C.; Dupont-Gillain, C.; Delcorte, A. Gas Cluster Ion Beams as a Versatile Soft-Landing Tool for the Controlled Construction of Thin (Bio)Films. *ACS Appl. Bio Mater.* **2022**, *5* (7), 3180−3192.
(12) Fu, T.; Della-Negra, S.; Touboul, D.; Brunelle, A. Internal Energy Distribution of Secondary Ions Under Argon and Bismuth Cluster Bombardments: "Soft" Versus "Hard" Desorption-Ionization Process. *J. Am. Soc. Mass Spectrom.* **2019**, *30* (2), 321−328.
(13) Lorenz, M.; Shard, A. G.; Counsell, J. D. P.; Hutton, S.; Gilmore, I. S. Angular Distribution of Molecules Sputtered by Gas Cluster Ion Beams and Implications for Secondary Neutral Mass Spectrometry. *J. Phys. Chem. C* **2016**, *120* (44), 25317−25327.
(14) Delcorte, A.; Poleunis, C. Mechanistic Insight into Gas Cluster-Induced Sputtering of Kilodalton Molecules Using Kinetic Energy Distribution Measurements. *J. Phys. Chem. C* **2019**, *123* (32), 19704−19714.
(15) Delcorte, A. A Microscopic View of Macromolecule Transfer in the Vacuum Using Gas and Bismuth Clusters. *J. Phys. Chem. C* **2022**, *126* (16), 7307−7318.
(16) Lorenz, M.; Zhang, J.; Shard, A. G.; Vorng, J. L.; Rakowska, P. D.; Gilmore, I. S. Method for Molecular Layer Deposition Using Gas Cluster Ion Beam Sputtering with Example Application in Situ Matrix-Enhanced Secondary Ion Mass Spectrometry. *Anal. Chem.* **2021**, *93* (7), 3436−3444.
(17) Moshkunov, K.; Tomasetti, B.; Daphnis, T.; Delmez, V.; Vanvarenberg, K.; Préat, V.; Lorenz, M.; Quanico, J.; Baggerman, G.; Lemiere, F.; Dupont, C.; Delcorte, A. Improvement of Biomolecular Analysis in Thin Films Using: In Situ Matrix Enhanced Secondary Ion Mass Spectrometry. *Analyst* **2021**, *146* (21), 6506−6519.
(18) Daphnis, T.; Tomasetti, B.; Delmez, V.; Vanvarenberg, K.; Préat, V.; Thieffry, C.; Henriet, P.; Dupont-Gillain, C.; Delcorte, A. Improvement of Lipid Detection in Mouse Brain and Human Uterine Tissue Sections Using In Situ Matrix Enhanced Secondary Ion Mass Spectrometry. *J. Am. Soc. Mass Spectrom.* **2023**, *34* (10), 2259−2268.
(19) Tomasetti, B.; Lauzin, C.; Delcorte, A. Enhancing Ion Signals and Improving Matrix Selection in Time-of-Flight Secondary Ion Mass Spectrometry with Microvolume Expansion Using Large Argon Clusters. *Anal. Chem.* **2023**, *95*, 13620−13628.
(20) Liuquan, C.; Michael, J. P. Mechanisms of Protein Stabilization in the Solid State. *J. Pharm. Sci.* **2009**, *98* (9), 2271−2280.
(21) Bertolini, S.; Delcorte, A. Unraveling the Molecular Dynamics of Glucose Oxidase Desorption Induced by Argon Cluster Collision. *J. Phys. Chem. B* **2023**, *127* (42), 9074−9081.
(22) Oran, U.; Ünveren, E.; Wirth, T.; Unger, W. E. S. Poly-Dimethyl-Siloxane (PDMS) Contamination of Polystyrene (PS) Oligomers Samples: A Comparison of Time-of-Flight Static Secondary Ion Mass Spectrometry (TOF-SSIMS) and X-Ray Photoelectron Spectroscopy (XPS) Results. *Appl. Surf. Sci.* **2004**, *227* (1−4), 318−324.
(23) Hageman, M. J. The role of moisture in protein stability. *Drug Dev. Ind. Pharm.* **1988**, *14* (14), 2047−2070.
(24) Bertolini, S.; Delcorte, A. Reactive Molecular Dynamics Simulations of Lysozyme Desorption under Ar Cluster Impact. *Appl. Surf. Sci.* **2023**, *631* (May), 157487.
(25) Becktel, W. J.; Schellman, J. A. Protein Stability Curves. *Biopolymers* **1987**, *26* (11), 1859−1877.
(26) Strucksberg, K. H.; Rosenkranz, T.; Fitter, J. Reversible and Irreversible Unfolding of Multi-Domain Proteins. *Biochim. Biophys. Acta Proteins Proteomics* **2007**, *1774* (12), 1591−1603.

https://doi.org/10.1021/acsami.4c06432
ACS Appl. Mater. Interfaces XXXX, XXX, XXX−XXX